

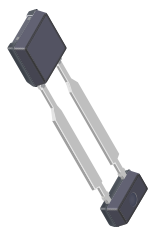
High-Resolution GMR Wheel Speed and Distance Sensor IC

FEATURES AND BENEFITS

- **High-resolution measurement** for enhanced ADAS accuracy, such as for automated parking
- **GMR technology** delivers high magnetic sensitivity for large air gaps and low-jitter switching
- **SolidSpeed Digital Architecture** provides robust, adaptive performance for high output accuracy and full-pitch vibration immunity
- **Integrated solution** includes the IC and a protection capacitor in a single overmolded package
- **ISO 26262 ASIL B(D)** with integrated diagnostics and certified safety design process



PACKAGE:



2-Pin SIP
(suffix UB)

Not to scale

DESCRIPTION

The A19360 is a magnetic sensor integrated circuit (IC) that uses giant magnetoresistance (GMR) technology to encode the speed and direction of rotating ring magnets. Innovative algorithms generate additional events per magnetic cycle while staying robust to air-gap variation, to provide high-resolution rotational data that can be used for accurate distance measurement. The A19360 is compatible with standard ring magnets used in automotive braking systems, and Allegro programs each IC according to the characteristics of the magnet used.

The A19360 is available in two resolution options (4 or 8 events per cycle) and two protocol options (pulse width or AK protocol). The four-event AK protocol option uses 28 mA speed pulses for every event and operates continuously throughout the full frequency range using standard bit truncation at higher speeds. The eight-event AK protocol option uses 14 mA speed pulses for high-resolution events and features an automatic crossover to standard resolution at higher speeds, maximizing the available bandwidth of the two-wire interface.

The A19360 was developed in accordance with ISO 26262 as a hardware safety element out of context, rated ASIL B(D) for use in automotive safety-related systems when integrated and used in the manner prescribed in the applicable safety manual and datasheet.

The A19360 is provided in a two-pin SIP package (suffix UB) that is lead (Pb) free, with tin lead frame plating. The UB package includes an IC and protection capacitor integrated into a single overmolded package, with an additional molded lead-stabilizing bar for robust shipping and ease of assembly.

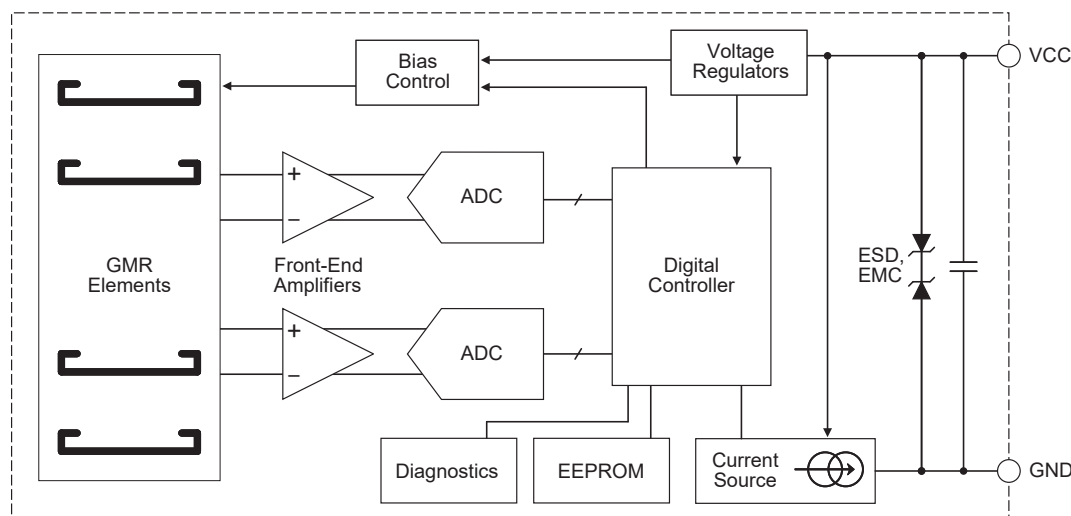


Figure 1: Functional Block Diagram

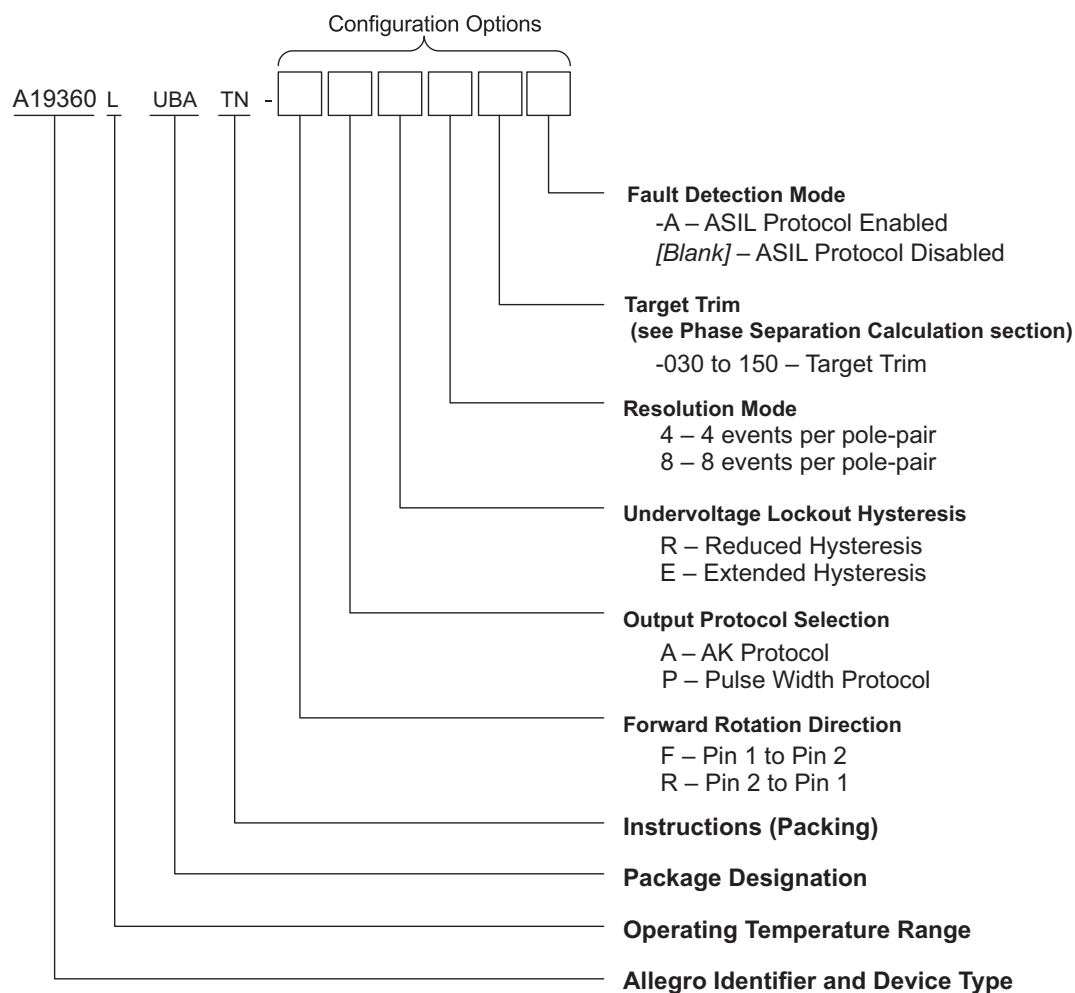
SELECTION GUIDE*

Part Number	Packing
A19360LUBATN-FAE4-065-A	Tape and Reel, 4000 pieces per reel

* Not all combinations are available. For availability and pricing of custom programming options, contact Allegro sales.



Complete Part Number Format



SPECIFICATIONS

ABSOLUTE MAXIMUM RATINGS

Characteristic	Symbol	Notes	Rating	Unit
Supply Voltage	V_{CC}	Refer to Power Derating section; potential between pin 1 and pin 2	28	V
Reverse Supply Voltage	V_{RCC}		−18	V
Operating Ambient Temperature	T_A		−40 to 150	°C
Maximum Junction Temperature	$T_{J(max)}$		175	°C
Storage Temperature	T_{stg}		−65 to 170	°C
Applied Magnetic Flux Density	B	In any direction	500	G

INTERNAL DISCRETE CAPACITOR RATINGS

Characteristic	Symbol	Test Conditions	Value	Unit
Nominal Capacitance	C_{SUPPLY}	Connected between pin 1 and pin 2 (refer to Figure 3)	2.2	nF

PINOUT DIAGRAM AND LIST

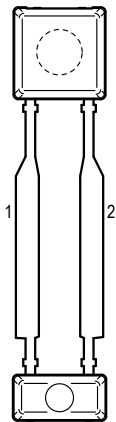


Figure 2: Package UB, Two-Pin SIP Pinout Diagram

Table 1: Pinout List

Pin Name	Pin Number	Function
VCC	1	Supply Voltage
GND	2	Ground

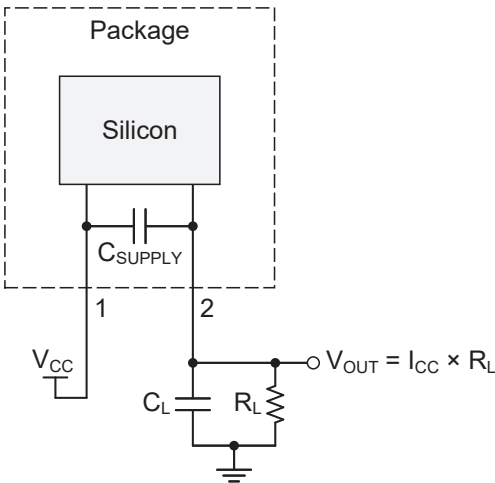


Figure 3: Typical Application Circuit

OPERATING CHARACTERISTICS: Valid throughout full operating voltage and temperature ranges, unless otherwise specified

Characteristic	Symbol	Test Conditions		Min.	Typ. [1]	Max.	Unit
ELECTRICAL CHARACTERISTICS							
Supply Voltage [2]	V _{CC}	Potential between pin 1 and pin 2	-xxRx variant [3]	4.25	–	24	V
			-xxEx variant	5.2	–	24	V
Undervoltage Lockout (UVLO)	V _{CC(OFF)}	V _{CC} switch off		–	–	3.5	V
UVLO Hysteresis	V _{HYS}	-xxRx variant		0.5	–	–	V
		-xxEx variant		1.5	–	–	V
Reverse Supply Current [4]	I _{RCC}	V _{CC} = V _{RCC(MAX)}		–10	–	–	mA
Supply Zener Clamp Voltage	V _{Zsupply}	I _{CC} = I _{CC(MAX)} + 3 mA		28	–	–	V
Supply Current	I _{CC(LOW)}	Low-current state		5.88	7	8.4	mA
	I _{CC(MID)}	Mid-current state		11.76	14	16.8	mA
	I _{CC(HIGH)}	High-current state		23.52	28	33.6	mA
Supply Current Ratio [5]		I _{CC(MID)} /I _{CC(LOW)} (isothermal)		1.9	–	–	–
		I _{CC(HIGH)} /I _{CC(LOW)} (isothermal)		3.8	–	–	–
Fault Current	I _{FAULT}	Refer to the figure in the Output Protocol in Fault Condition section		1	–	3.8	mA
Fault Current Duration	t _{W(FAULT)}	Refer to the figure in the Output Protocol in Fault Condition section		4	–	7	ms
Output Rise, Fall Slew Rate	SR	R _L = 50 Ω, C _L = 10 pF, measured between 10% and 90% of signal		8	–	28	mA/μs
POWER-ON CHARACTERISTICS							
Power-On State	POS	V _{CC} > V _{CC(min)} , as connected in Figure 3		I _{CC(LOW)}			mA
Power-On Time [6]	t _{PO}	V _{CC} > V _{CC(min)} , as connected in Figure 3		–	–	1	ms
Calibration Time	T _{CAL}	Post t _{PO} time to first AK protocol output event (f < 200 Hz)	-xAx8 variant	–	0.75	1.25	T _{CYCLE}
			-xAx4 variant	–	1	1.5	T _{CYCLE}
		Post t _{PO} time to first valid direction event (f < 200 Hz)	-xxx8 variant	–	0.75	1.25	T _{CYCLE}
			-xxx4 variant	–	1	1.5	T _{CYCLE}

[1] Typical values are at $T_A = 25^\circ\text{C}$ and $V_{CC} = 12 \text{ V}$. Performance may vary for individual units, within the specified maximum and minimum limits.

[2] Maximum voltage must be adjusted for power dissipation and junction temperature; see representative Power Derating section.

[3] Part switching may cause the part to re-enter UVLO when this option is used with the AK protocol and a 50Ω load.

[4] Negative current is defined as conventional current coming out of (sourced from) the specified device terminal.

[5] Supply current ratios are taken as the mean value of $I_{CC(MID)} / I_{CC(LOW)}$ and the mean value of $I_{CC(HIGH)} / I_{CC(LOW)}$, respectively.

[6] Time between power-on to I_{CC} stabilizing; output transients prior to t_{PO} should be ignored.

Continued on the next page...

OPERATING CHARACTERISTICS (continued): Valid throughout full operating voltage and temperature ranges, unless otherwise specified

Characteristic	Symbol	Test Conditions	Min.	Typ. [1]	Max.	Unit
INPUT CHARACTERISTICS AND PERFORMANCE						
Operating Single-Ended Magnetic Input Signal [7]	B_{SE}	Combined single-element signal and offset must fall within this range.	-100	—	100	G
Operating Differential Magnetic Input Signal [7]	$B_{DIFF(pk-pk)}$	Peak-to-peak of differential magnetic input (refer to Figure 7)	5	—	400	G
Allowable User-Induced Differential Offset	$B_{DIFFEXT}$	External differential signal bias (DC), operating within specification	-20	—	20	G
Operating Magnetic Input Signal Variation	$\Delta B_{DIFF(pk-pk)}$	Bounded amplitude ratio within T_{WINDOW} [8]; no missed output transitions or flat-line condition; possible incorrect direction data; see Figure 5 and Figure 6	0.6	—	—	—
Operating Magnetic Input Signal Window	T_{WINDOW}	Rolling window where $\Delta B_{DIFF(pk-pk)}$ cannot exceed bounded ratio; see Figure 5 and Figure 6	5	—	—	T_{CYCLE}
Operate Point	B_{OP}	% of peak-to-peak IC-processed signal	—	60	—	%
Release Point	B_{RP}	% of peak-to-peak IC-processed signal	—	40	—	%
Repeatability [9]	$Err_{\theta E}$	Constant air gap, temperature, and target speed. $B_{DIFF(pk-pk)} > 20 G_{(pk-pk)}$. Primary pulses, percent of a T_{CYCLE} one sigma	—	—	0.05	%
		Constant air gap, temperature, and target speed. $B_{DIFF(pk-pk)} > 20 G_{(pk-pk)}$. High-resolution pulses, one sigma	—	—	0.085	%
Phase Separation	Φ_P	For calculations, refer to the Phase Separation Calculation section	30	—	150	degrees
OUTPUT CHARACTERISTICS (-XPX8 VARIANT)						
Pulse-Width Off Time	$t_{W(PRE)}$	Enforced signal-low duration	25	30	36	μs
Forward Pulse Width	$t_{W(FWD)}$	Magnetic input frequency $< f_{L,PW}$	38	45	52	μs
Reverse Pulse Width	$t_{W(REV)}$	Magnetic input frequency $< f_{L,PW}$	76	90	104	μs
High-Speed Pulse Width	$t_{W(HS)}$	Magnetic input frequency $> f_{H,PW}$	25	30	36	μs
Standstill Pulse Width	$t_{W(STILL)}$		1232	1440	1656	μs
Standstill Period	t_{STOP}		590	737	848	ms
Low-to-High Speed Threshold	$f_{H,PW}$	Frequency at which device transitions to high-speed operation (increasing frequency)	850	1000	1150	Hz
High-to-Low Speed Threshold	$f_{L,PW}$	Frequency at which device transitions to low-speed operation (decreasing frequency)	800	950	1100	Hz
Speed Threshold Hysteresis	$f_{HYS,PW}$		—	50	—	Hz
Operating Frequency, High-Speed Pulses [10]	f_{HS}		0	—	4	kHz

[7] Differential magnetic field measured for Channel A (E1 – E3) and Channel B (E2 – E4). The differential magnetic field of each channel is measured between two GMR elements spaced by 1.5 mm. Magnetic field is measured in the B_y direction and the $|B_x|$ field must be less than 80 G (refer to Figure 8).

[8] Symmetrical signal variation is defined as the largest amplitude ratio from B_n to $B_n + T_{WINDOW}$. Signal variation may occur continuously while B_{DIFF} remains in the operating magnetic range.

[9] Greater than 1000 output edges captured. Repeatability (i.e., jitter) is tested to 1 sigma and guaranteed by design and characterization only.

[10] Frequency is based on B_{DIFF} frequency.

Continued on the next page...

OPERATING CHARACTERISTICS (continued): Valid throughout full operating voltage and temperature ranges, unless otherwise specified

Characteristic	Symbol	Test Conditions	Min.	Typ. [1]	Max.	Unit
OUTPUT CHARACTERISTICS (-XPX4 VARIANT)						
Pulse-Width Off Time	$t_{W(PRE)}$	Enforced signal-low duration	25	30	36	μs
Forward Pulse Width	$t_{W(FWD)}$		38	45	52	μs
Reverse Pulse Width	$t_{W(REV)}$		76	90	104	μs
Standstill Pulse Width	$t_{W(STILL)}$		1232	1440	1656	μs
Standstill Period	t_{STOP}		590	737	848	ms
Operating Frequency, Forward Pulses [10]	f_{FWD}		0	–	3.3	kHz
Operating Frequency, Reverse Pulses [10]	f_{REV}		0	–	2.2	kHz
OUTPUT CHARACTERISTICS (-XAX8 VARIANT)						
Bit Width	t_p		40	50	60	μs
Standstill Period	t_{STOP}		105	150	195	ms
Post-Standstill Suppression Delay	t_{PSSD}	High-resolution pulse delay when truncating a standstill pulse	300	400	–	μs
Pulse-Width Off Time	$t_{W(PRE)}$		–	75	–	μs
Low-to-High Speed Threshold	$f_{H,AK}$	Frequency at which device transitions to high-speed operation (increasing frequency)	170	200	230	Hz
High-to-Low Speed Threshold	$f_{L,AK}$	Frequency at which device transitions to low-speed operation (decreasing frequency)	160	190	220	Hz
Speed Threshold Hysteresis	$f_{HYS,AK}$		–	10	–	Hz
Air-Gap Reserve Level	B_{LR}	Signal amplitude that engages AK LR bit	–	5	–	G
Operating Frequency [10]	f_{SIG}		0	–	4	kHz
OUTPUT CHARACTERISTICS (-XAX4 VARIANT)						
Bit Width	t_p		40	50	60	μs
Standstill Period	t_{STOP}		105	150	195	ms
Pulse-Width Off Time	$t_{W(PRE)}$		–	75	–	μs
Air-Gap Reserve Level	B_{LR}	Signal amplitude that engages AK LR bit	–	5	–	G
Operating Frequency [10]	f_{SIG}		0	–	2.5	kHz
THERMAL CHARACTERISTICS						
Magnetic Temperature Coefficient [11]	TC	Based on ferrite	–	0.2	–	%/°C
Package Thermal Resistance	$R_{\theta JA}$	Single-layer PCB with copper limited to solder pads	–	213	–	°C/W
PERFORMANCE CHARACTERISTICS						
Vibration Detection	N_{VIB_CHANGE}	Number of direction changes until vibration is detected	–	4	–	–
Vibration Release	T_{VIB_CONST}	Number of consecutive constant-direction pulses to release vibration count and suppression	–xxx8 variant	–	8	–
			–xxx4 variant	–	4	–

[11] Ring magnet decreases in magnetic strength with rising temperature, and the device compensates. Note that the $B_{DIFF(pk-pk)}$ requirement is not influenced by this.

OPERATING CHARACTERISTICS (continued): Valid throughout full operating voltage and temperature ranges, unless otherwise specified

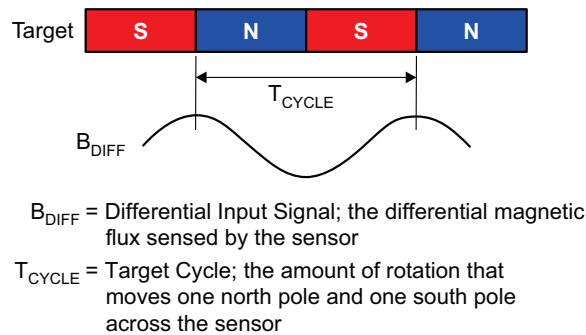


Figure 4: Definition of T_{CYCLE}

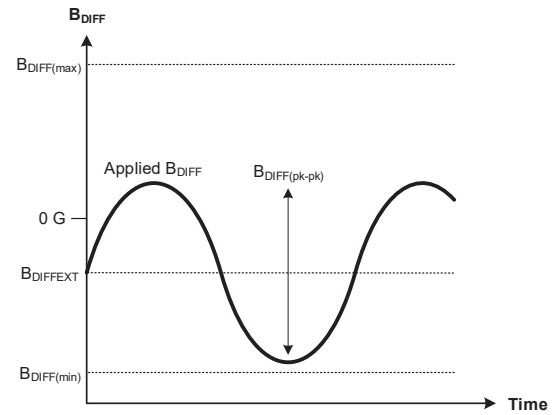


Figure 5: Input Signal Definition

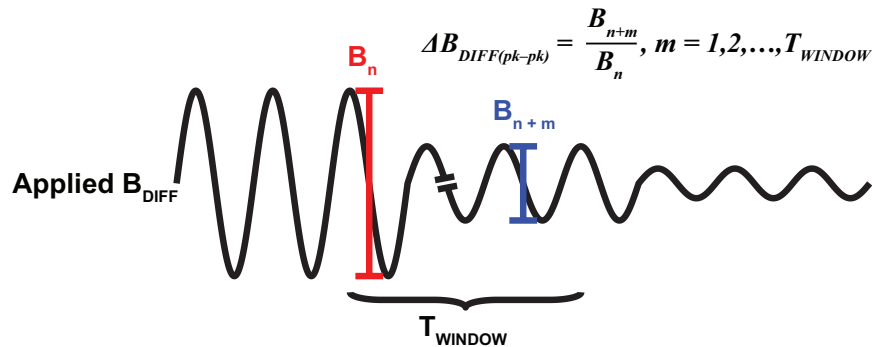


Figure 6: Single Period-to-Period Variation

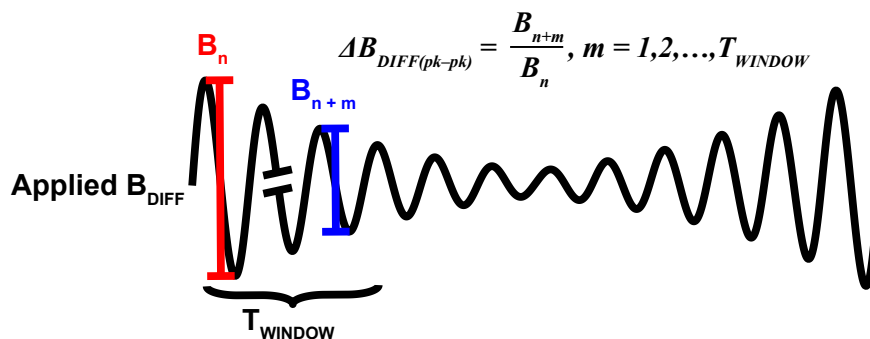


Figure 7: Repeated Period-to-Period Variation

FUNCTIONAL DESCRIPTION

The A19360 sensor IC contains a single-chip GMR circuit that uses spaced elements. These elements are used in differential pairs to provide electrical signals containing data regarding edge position and direction of rotation. The A19360 is intended for use with ring-magnet targets, as shown in Figure 9. The IC detects the peaks of the magnetic signals and sets dynamic thresholds based on these detected signals.

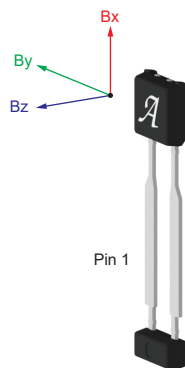


Figure 8: Package Orientation

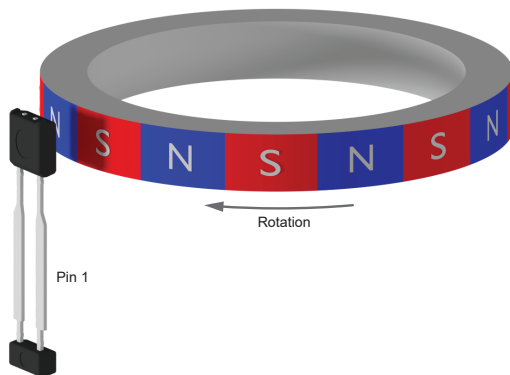


Figure 9: Sensing Orientation

Phase-Separation Calculation

The A19360 is compatible with a wide range of ring-magnet targets, according to the supported phase-separation range. For each target and air gap, the channel-to-channel phase separation can be calculated using:

$$\Phi_p = \frac{360}{2\pi} \times \frac{1.085 \text{ mm} \times N_{pp}}{r_{\text{target}} + d_{AG}}$$

where Φ_p is the channel-to-channel phase separation, N_{pp} is the number of pole-pairs the target has, r_{target} is the target radius in mm, and d_{AG} is the nominal air gap for radial sensed targets in mm or unused for axial sensed targets.

Each A19360 is trimmed to a specific target encoder, which is indicated by the “Target Trim” in the selection guide. Correct trimming is required for accurate output data and performance, including output event phase accuracy, direction detection, and vibration detection.

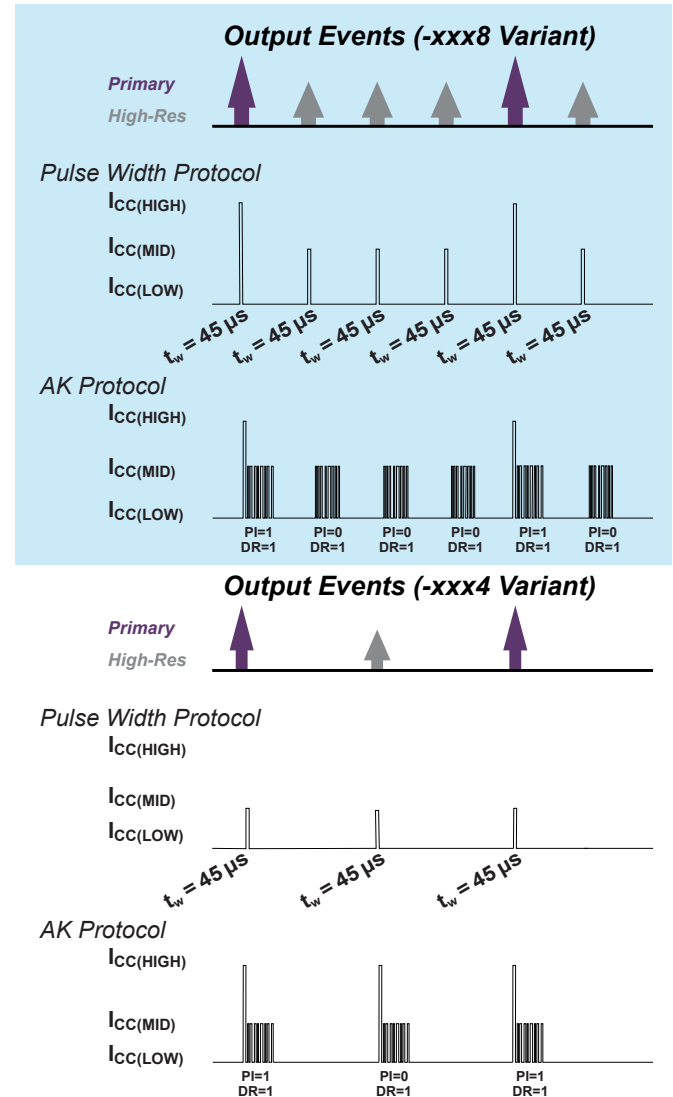
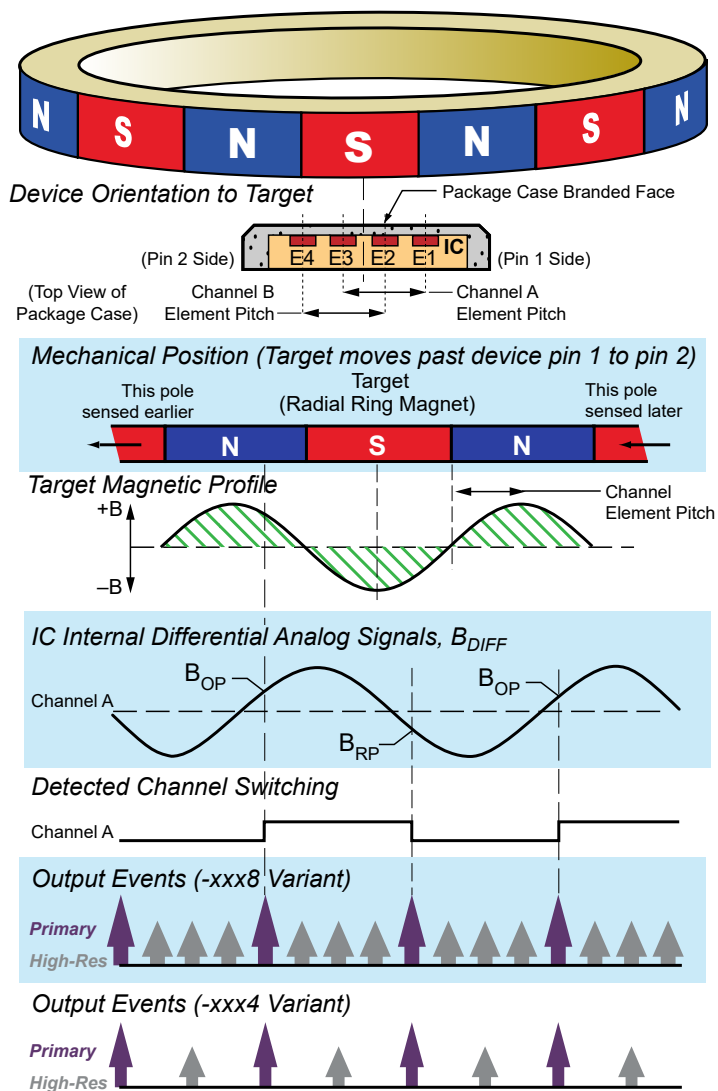


Figure 10: Basic Operation

Forward Rotation

For the -Fxxx variant, when the target is rotating such that a target feature passes from pin 1 to pin 2, this is referred to as forward rotation. For the -Rxxx variant, forward rotation is indicated when a target feature passes from pin 2 to 1.

Reverse Rotation

For the -Fxxx variant, when the target is rotating such that a target feature passes from pin 2 to pin 1, this is referred to as reverse rotation. For the -Rxxx variant, reverse rotation is indicated when a target feature passes from pin 1 to 2.

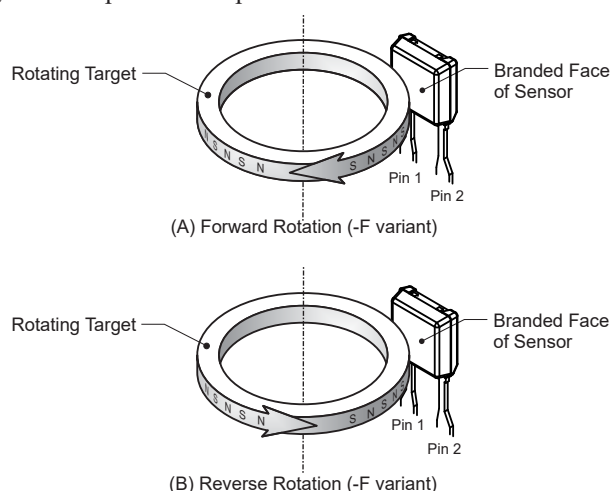


Figure 11: Target Orientation Relative to Device

AK Protocol

When a target passes in front of the device (opposite the branded face of the package), the A19360 generates output words that are triggered by B_{DIFF} transitions through equidistant switch points. On a switch-point crossing, the speed pulse and relevant data are generated and transmitted. The IC is capable of properly detecting input signals up to the defined operating frequency. Speed data are provided by the speed pulse rate, and other data are directly communicated via the AK bits.

The -xxx8 variant generates eight output words—two primary words and six high-resolution words—for each magnetic pole-pair of the target when it is rotating at low speeds below the $f_{L,AK}$ threshold. At higher rotating speeds above the $f_{H,AK}$ threshold, this variant automatically switches to standard resolution and only outputs two primary words per pole-pair. Primary words are generated with a speed pulse current of $I_{CC(HIGH)}$ while high-resolution words are generated with a speed pulse current of $I_{CC(MID)}$.

The -xxx4 variant generates four output words—two primary words and two high-resolution words—for each magnetic pole-pair of the target. This variant outputs four output words for all operating frequencies. Both primary and high-resolution words are generated with a speed pulse current of $I_{CC(HIGH)}$.

For further information, refer to Description of AK Protocol.

Pulse Width Protocol

When a target passes in front of the device (opposite the branded face of the package), the A19360 generates output pulses that are triggered by B_{DIFF} transitions through equidistant switch points. On a switch-point crossing, the corresponding direction pulse is generated and transmitted. Speed data are provided by the speed pulse rate, and the direction of the target rotation data is provided by the pulse width.

The -xxx8 variant generates eight output pulses—two primary pulses and six high-resolution pulses—for each magnetic pole-pair of the target when it is rotating at low speed below the $f_{L,PW}$ threshold. At higher rotating speed above the $f_{H,PW}$ threshold, this variant automatically switches to standard resolution and only outputs two primary pulses per pole-pair. Primary pulses are generated with a pulse current of $I_{CC(HIGH)}$ while high-resolution pulses are generated with a pulse current of $I_{CC(MID)}$.

The -xxx4 variant generates four output pulses—two primary pulses and two high-resolution pulses—for each magnetic pole-pair of the target. This variant outputs four output pulses for all operating frequencies. Both primary and high-resolution pulses are generated with a speed pulse current of $I_{CC(MID)}$.

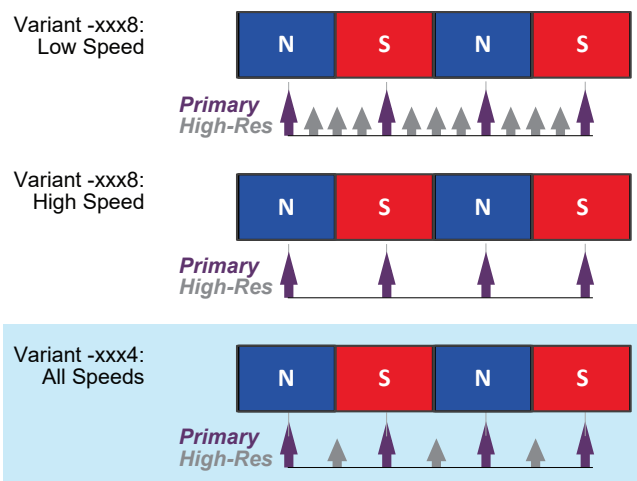


Figure 12: Output Events

Description of AK Protocol

The A19360 fulfills requirements according to the AK Protocol specification “Requirement Specification for Standardized Interface for Wheel Speed Sensors with Additional Information ‘AK-Protokoll’” version 4.0, with some modifications, as discussed in the sections that follow.

AK Bit Definitions

The AK word consists of 10 pulses—a single speed pulse, 8 data bits, and a single parity bit. The speed pulse and data bit definitions are described in Table 2.

LM/HR Data Bits Decoding

The -xAx8 variant of the A19360 outputs air-gap indication (LM) data on bits [5:7] if the generated pulse is a primary pulse. If the generated pulse is a high-resolution (HR) pulse, bits [5:7] report which HR pulse generated the output event.

The -xAx4 variant of the A19360 outputs air-gap indication (LM) data on bits [5:7] on all generated pulses. HR data are unused.

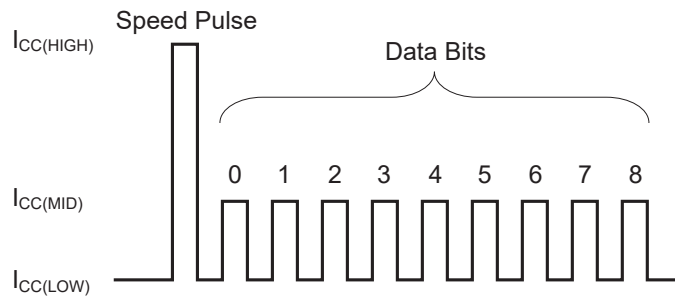


Figure 13: Speed Pulse and Data Bits

Table 2: Speed Pulse and Data Bit Definitions

Bit Number	Field	Abbr.	Coding	Post-Power-On Default Value
–	Speed Pulse	SP	$I_{CC(HIGH)}$ if primary or high-resolution pulse, $I_{CC(MID)}$ if standstill pulse (-xAx4 variant) $I_{CC(HIGH)}$ if primary pulse, $I_{CC(MID)}$ if high-resolution or standstill pulse (-xAx8 variant)	–
0	Air Gap Reserve	LR	1 if $B_{DIFF(pk-pk)} < B_{LR(pk-pk)}$, 0 otherwise	0
1	Status Mode	M	1 if running mode is not active, 0 otherwise	1
2	Primary Indication	PI	1 if primary or standstill pulse, 0 if high-resolution pulse	1
3	Direction Validity	GDR	1 if direction is valid, 0 otherwise	0
4	Direction	DR	1 if forward rotation, 0 if reverse rotation	0
5	Air Gap Indication or High-Resolution Pulse (LSB)	LM0/HR0	LM/HR LSB	0
6	Air Gap Indication or High-Resolution Pulse	LM1/HR1	LM/HR	0
7	Air Gap Indication of High-Resolution Pulse (MSB)	LM2/HR2	LM/HR MSB	0
8	Parity	P	1 if parity incl. parity bit is even, 0 otherwise	0

LM Air Gap Table

Data bits [5:7] report the air-gap indication. These bits give eight air-gap ranges with respect to the measured peak-to-peak magnetic field, $B_{DIFF(pk-pk)}$.

Table 3: Data Bits [5:7]—Air Gap Indications

LM2	LM1	LM0	$B_{DIFF(pk-pk)}$ Range (Typ.)
0	0	0	< 5.6 G
0	0	1	5.6 to 11 G
0	1	0	11 to 22 G
0	1	1	22 to 45 G
1	0	0	45 to 90 G
1	0	1	90 to 180 G
1	1	0	180 to 360 G
1	1	1	> 360 G

Data bits [5:7] report which HR pulse was generated. These bits allow for up to eight unique pulse labels, so each HR pulse has a unique label.

Table 4: Data Bits [5:7]—HR Pulses

HR2	HR1	HR0	Description
0	0	0	Unused
0	0	1	HR pulse 1
0	1	0	HR pulse 2
0	1	1	HR pulse 3
1	0	0	Unused
1	0	1	HR pulse 4
1	1	0	HR pulse 5
1	1	1	HR pulse 6

Standstill

If no pulses are output for t_{STOP} , in the -xAxx variant of the A19360, a standstill pulse is generated. The standstill event is always generated with an $I_{CC(MID)}$ speed pulse. For the -xAx8 variant, where high-resolution pulses are also generated with an $I_{CC(MID)}$ pulse, the A19360 delays the high-resolution pulse by t_{PSSD} if a high-resolution pulse truncates a standstill pulse.

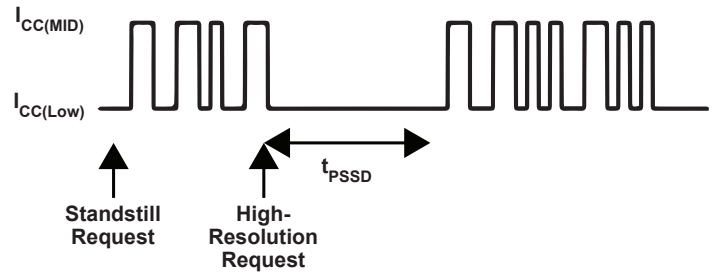


Figure 14: $I_{CC(MID)}$ Pulse-Truncating Standstill Pulse Example, -xAx8 Variant

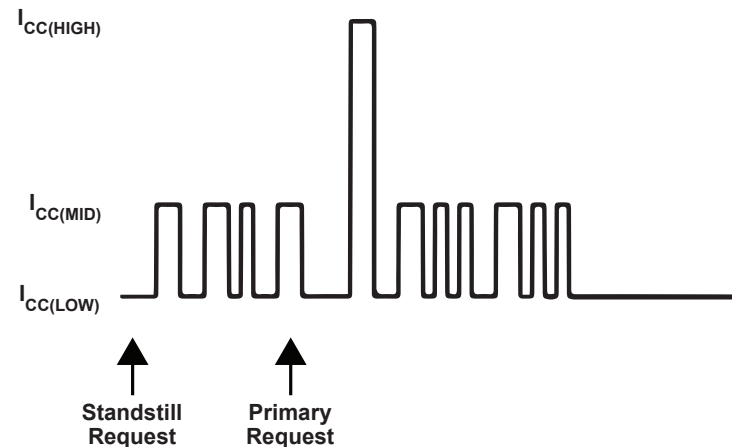


Figure 15: $I_{CC(HIGH)}$ Pulse-Truncating Standstill Pulse Example

Output Protocol in Fault Condition

The A19360 sensor IC contains diagnostic circuitry that continuously monitors occurrences of failure defects within the IC. For the output protocol after a fault has been detected, refer to Figure 16.

NOTE: If a fault exists continuously, the device output remains at the I_{FAULT} level. For additional details, refer to the A19360 Safety Manual.

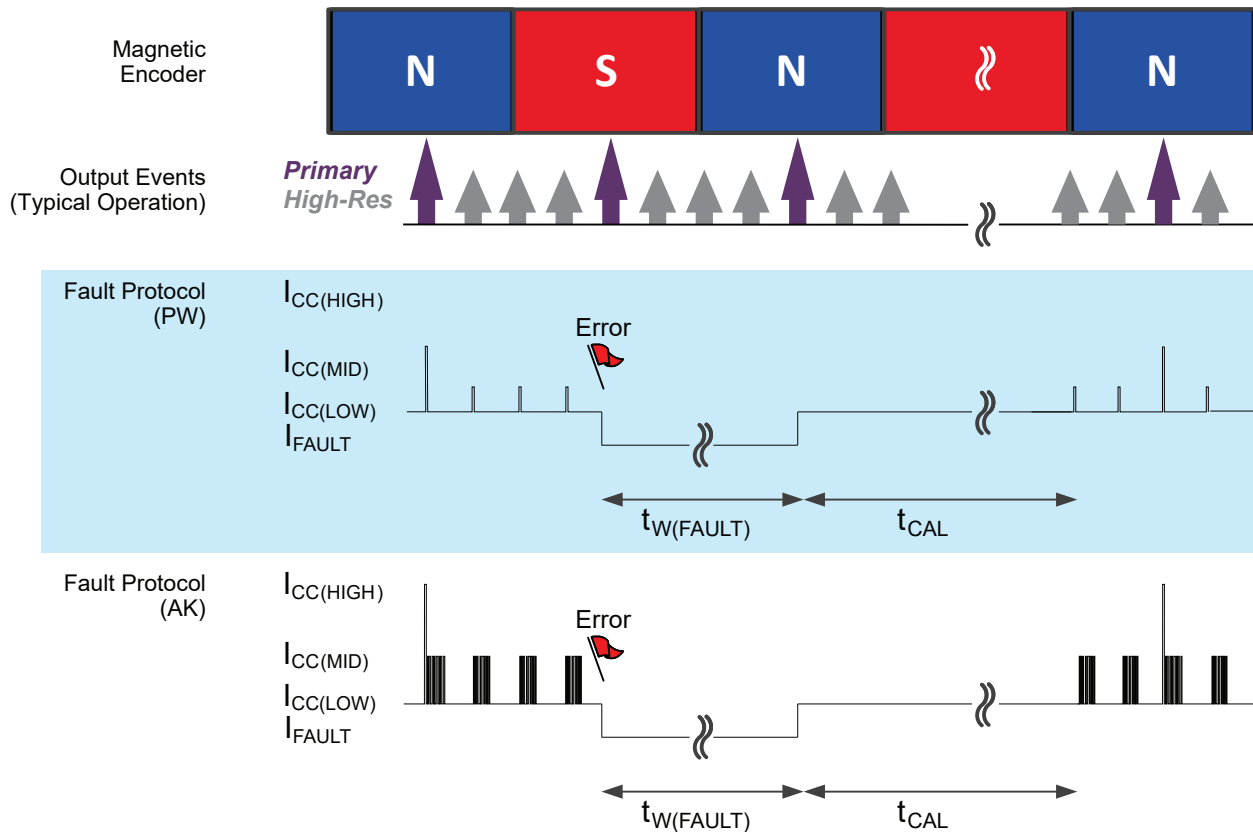


Figure 16: Output Protocols in Fault Condition

Calibration and Direction Validation

When power is applied to the A19360, the built-in algorithm performs an initialization routine. For a short period after power-on, the device calibrates itself and determines the direction of target

rotation. Once the calibration routine is complete, the A19360 transmits accurate speed and direction data via the selected output protocol.

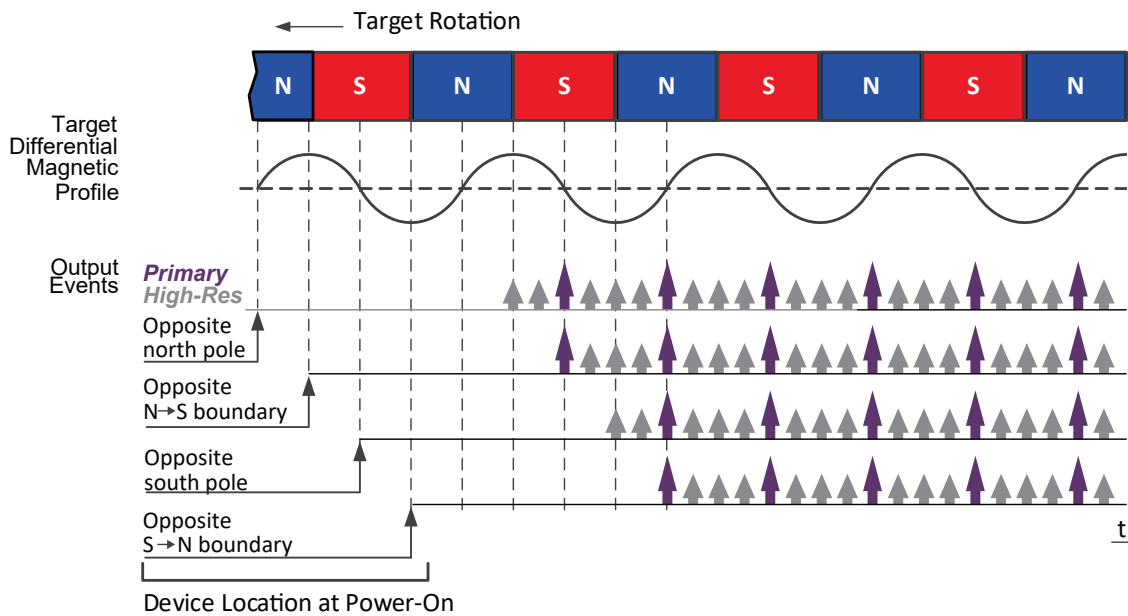


Figure 17: Calibration Behavior

Direction Changes, Vibrations, and Anomalous Events

During operation, the A19360 is exposed to changes in the direction of target rotation (Figure 18), vibrations of the target (Figure 19), and anomalous events such as sudden air-gap changes. The A19360 has built-in vibration algorithms that detect and blank pulses if the directional changes of N_{VIB_CHANGE} occur without the T_{VIB_CONST} consecutive constant direction pulses between each direction change. Vibration detection exits when T_{VIB_CONST} consecutive direction events occur.

During a vibration event, the last reported direction before blanking begins depends on the magnetic angle where vibration began. As the -xxx4 variant detects vibration at a higher resolution than output events, vibration may be entered after consecutive direction events are outputted.

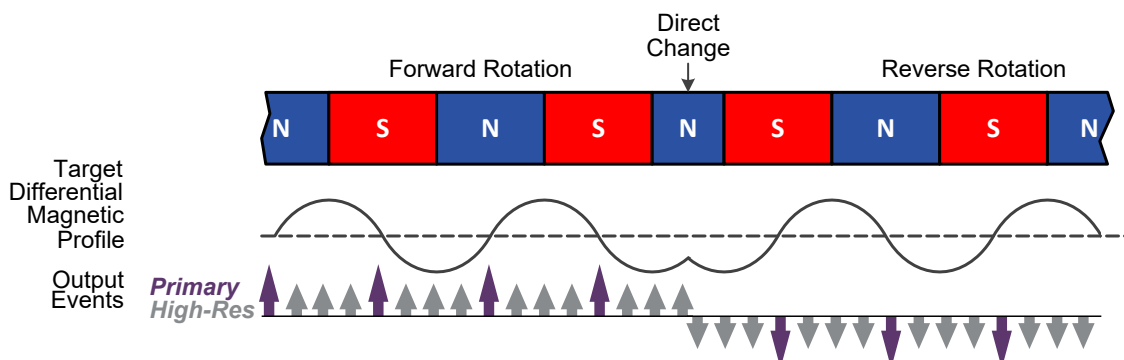


Figure 18: Direction Change Behavior

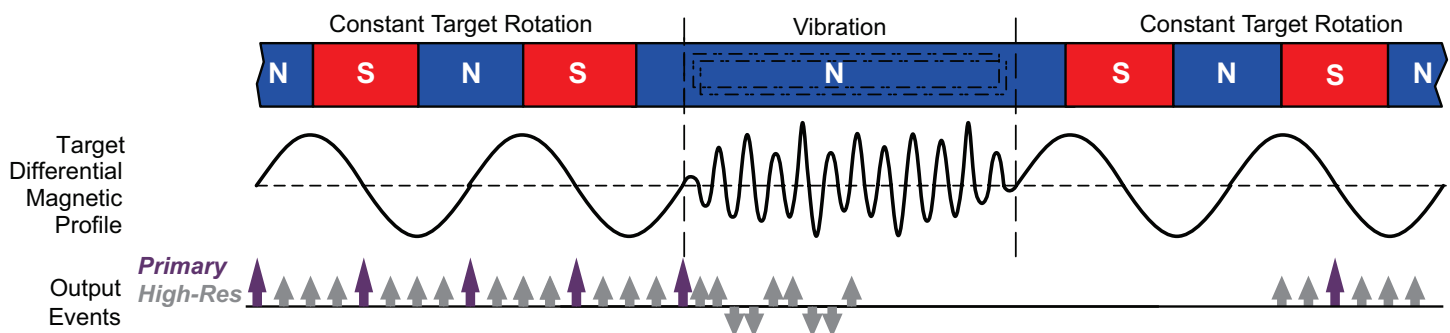


Figure 19: Vibration Behavior

POWER DERATING

The device must be operated below the maximum junction temperature of the device, $T_{J(max)}$. Under certain combinations of peak conditions, reliable operation may require derating supplied power or improving the heat dissipation properties of the application. This section presents a procedure for correlating factors affecting operating T_J . (Thermal data is also available on the Allegro MicroSystems website.)

The package thermal resistance, $R_{\theta JA}$, is a figure of merit summarizing the ability of the application and the device to dissipate heat from the junction (die), through all paths to the ambient air. Its primary component is the effective thermal conductivity, K , of the printed circuit board, including adjacent devices and traces. Radiation from the die through the device case, $R_{\theta JC}$, is a relatively small component of $R_{\theta JA}$. Ambient air temperature, T_A , and air motion are significant external factors, damped by overmolding.

The effect of varying power levels (power dissipation, P_D) can be estimated. The following formulas represent the fundamental relationships used to estimate T_J , at P_D .

$$P_D = V_{IN} \times I_{IN} \quad (1)$$

$$\Delta T = P_D \times R_{\theta JA} \quad (2)$$

$$T_J = T_A + \Delta T \quad (3)$$

For example, given common conditions such as:

$T_A = 25^\circ\text{C}$, $V_{CC} = 12\text{ V}$, $I_{CC} = 7.15\text{ mA}$, and $R_{\theta JA} = 213^\circ\text{C/W}$, then:

$$P_D = V_{CC} \times I_{CC} = 12\text{ V} \times 7.15\text{ mA} = 85.8\text{ mW}$$

$$\Delta T = P_D \times R_{\theta JA} = 85.8\text{ mW} \times 213^\circ\text{C/W} = 18.3^\circ\text{C}$$

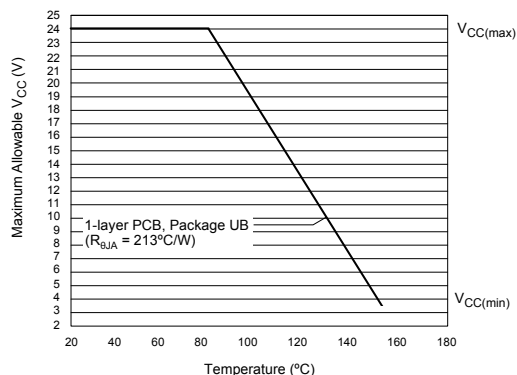


Figure 20: Power Derating Curve

$$T_J = T_A + \Delta T = 25^\circ\text{C} + 18.3^\circ\text{C} = 43.3^\circ\text{C}$$

A worst-case estimate, $P_{D(max)}$, represents the maximum allowable power level ($V_{CC(max)}$, $I_{CC(max)}$), without exceeding $T_{J(max)}$, at a selected $R_{\theta JA}$ and T_A .

Example: Reliability for V_{CC} at $T_A = 150^\circ\text{C}$.

Observe the worst-case ratings for the device, specifically:

$R_{\theta JA} = 213^\circ\text{C/W}$ (subject to change), $T_{J(max)} = 175^\circ\text{C}$, $V_{CC(max)} = 24\text{ V}$, and $I_{CC(AVG)} = 21\text{ mA}$. $I_{CC(AVG)}$ is computed using $I_{CC(HIGH)(max)}$ and $I_{CC(LOW)(max)}$, with a duty cycle of 50% computed from $f_{sig(max)}$ for the -xAX4 variant.

To calculate the maximum allowable power level, $P_{D(max)}$, first rearrange Equation 3:

$$\Delta T_{max} = T_{J(max)} - T_A = 175^\circ\text{C} - 150^\circ\text{C} = 25^\circ\text{C}$$

This provides the allowable increase to T_J resulting from internal power dissipation. Then, rearrange Equation 2:

$$P_{D(max)} = \Delta T_{max} \div R_{\theta JA} = 25^\circ\text{C} \div 213^\circ\text{C/W} = 117.4\text{ mW}$$

Finally, solve Equation 1 with respect to voltage:

$$V_{CC(est)} = P_{D(max)} \div I_{CC(max)} = 117.4\text{ mW} \div 21\text{ mA} = 5.6\text{ V}$$

The result indicates that, at T_A , the application and device can dissipate adequate amounts of heat at voltages $\leq V_{CC(est)}$.

Compare $V_{CC(est)}$ to $V_{CC(max)}$. If $V_{CC(est)} \leq V_{CC(max)}$, then reliable operation between $V_{CC(est)}$ and $V_{CC(max)}$ requires enhanced $R_{\theta JA}$. If $V_{CC(est)} \geq V_{CC(max)}$, then operation between $V_{CC(est)}$ and $V_{CC(max)}$ is reliable under these conditions.

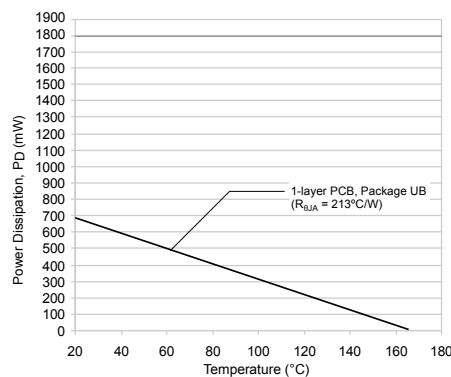


Figure 21: Power Dissipation versus Ambient Temperature

For Reference Only – Not for Tooling Use

Dimensions in millimeters – NOT TO SCALE

Exact case and lead configuration at supplier discretion within limits shown



Revision History

Number	Date	Description
–	November 29, 2021	Initial release
1	August 16, 2022	Updated Fault Current Duration symbol (page 4)
2	December 6, 2022	Updated Selection Guide table and Part Numbering Schematic (page 2); updated Phase Separation Calculation section (page 8)
3	January 26, 2024	Updated per revised technical style guidelines: changed future tense to present tense, removed or changed “normal” to “typical” or “constant,” minimized use of capitalization, added hyperlinks to internal cross-references, and made minor editorial changes throughout (all pages)
4	April 25, 2024	Updated package drawing (page 17)
5	August 6, 2024	Updated ASIL assessment status (page 1)

Copyright 2024, Allegro MicroSystems.

Allegro MicroSystems reserves the right to make, from time to time, such departures from the detail specifications as may be required to permit improvements in the performance, reliability, or manufacturability of its products. Before placing an order, the user is cautioned to verify that the information being relied upon is current.

Allegro’s products are not to be used in any devices or systems, including but not limited to life support devices or systems, in which a failure of Allegro’s product can reasonably be expected to cause bodily harm.

The information included herein is believed to be accurate and reliable. However, Allegro MicroSystems assumes no responsibility for its use; nor for any infringement of patents or other rights of third parties which may result from its use.

Copies of this document are considered uncontrolled documents.

For the latest version of this document, visit our website:

www.allegromicro.com